Publishing House
AKAPIT

COMPUTER METHODS IN MATERIALS SCIENCE

Informatyka w Technologii Materiałów

Vol. 13, 2013, No. 1

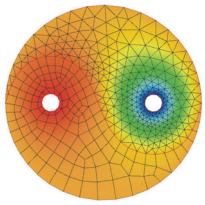

MATHEMATICAL MODELLING OF IRON ORE SINTERING PROCESS USING GENETIC ALGORITHM: EFFECT OF MOISTURE EVAPORATION AND CONDENSATION ON THE TEMPERATURE PROFILE

SEKHAR SUMAN, BRIJESH K. GIRI, GOUR G. ROY*

Department of Metallurgical & Materials Engineering, Kharagpur: 721 302, India
**Corresponding author: ggroy@metal.iitkgp.ernet.in*

Abstract

Sintering is a process where iron ore fines are agglomerated in the form of sinter cake by partial fusion in presence of fuel and flux. During sintering, the sinter bed is ignited from the top and the flame-front/fire-line is drawn through the bed under the action moving air. Estimation of the speed of flame-front progress through the sinter bed is of importance because efficiency of the sinter strand depends on the knowledge when the fire-line reaches just at the bottom of the bed. In the present article, a mathematical model of iron ore sintering process in a fixed sinter bed has been described, where Genetic algorithm has been used in conjunction with the process model for selecting the optimized process parameters. Presence of moisture influence the temperature profile significantly, because evaporation and condensation of moisture have effects both on the heat effects, and more importantly on the gas flow rate through the bed. The present article is a modification over the existing model of the present authors, where the effects of moisture condensation and evaporation have been introduced in the sinter model to account for the moisture effects explicitly. The results from this modified model clearly indicate marked improvement in the model predictions when the effect of moisture evaporation and condensation are taken into consideration.

Key words: sintering, genetic algorithm, fire-line, effect of moisture, optimization

1. INTRODUCTION

Sintering is a process where iron ore fines are converted into an agglomerated mass for charging into Blast Furnace. During sintering process, iron ore fines, along with coke breeze, limestone/lime, is granulated in presence of moisture in a rotary drum followed by sintering on a moving sinter strand. The sinter strand is ignited from the top and hot air is sucked through the bed. The fuel burns at a certain depth at certain time leading to a high temperature (~1300^{o}C) at combustion zone (also called flame-front/fire-line) that leads to stronger bonds between the particles through the formation of glass/ferrites (Biswas, 1981). The fire-line moves down through the bed with time or along the length of the sinter strand. During sintering, the fire-line should end just at the bottom of the bed at the exit end of the sinter strand for optimum process efficiency. The arrival of the fire-line at the bottom of the bed is indicated by the peak temperature in the wind box, known as the burn through point (BTP). An early arrival of BTP in the strand causes loss in productivity, while non-arrival of BTP at the exit end produces return sinters. Therefore, it is essential to correlate the dynamic position of the flame-front with the sintering parameters, like moisture, size and content of coke breeze, composition and blending of iron ores, etc.

 ISSN 1641-8581

In this regard, mathematical modelling can be an invaluable tool for analysing, controlling and optimising a complex process. Several transport phenomena based models have been reported in the literature, which have been summarised elsewhere (Venkataramana et al., 1998). In reported literature, even with very comprehensive models, deviations in temperature predictions are significant, especially on the cooling side. This is possibly due to the fact that the thermo-physical properties change significantly across the fire line because of marked change of the phase constituents across the fire line, which has not been considered in these models. As a first step towards this goal, Giri and Roy (2011) has already made an initial foundation of this model where process parameters above and below the fire-line have been tuned using a heuristic optimisation tool, genetic algorithm (GA). They started with simpler process model by considering only two major phenomena like gas-solid heat exchange and carbon combustion equation to predict the movement of fire line in a batch sintering machine. In the present study effect of moisture in the form of moisture evaporation and condensation has also been added in the phenomenological model to account for the effect of moisture explicitly.

2. MATHEMATICAL MODEL

2.1. Sinter model

One-dimensional unsteady state heat and mass transport is considered in the present model. This is because the relevant gas properties such as temperature, velocity, concentrations of oxygen, carbon dioxide and water vapour, hardly vary along the transverse section of the bed. The properties associated with solids, such as temperature, weight fractions of moisture, coke breeze, limestone and melt and the apparent density of solids, change with time (or along the length of the strand in case of a moving sinter strand). The process is governed by the following set of equations (1)–(10).

Energy balance for gas phase:

$$\dot{m}_g C_{pg} \frac{\partial T_g}{\partial z} = h a_s (T_s - T_g) + R_w \Delta H_w \quad (1)$$

Energy balance for solids:

$$\rho_s C_{ps} \frac{\partial T_s}{\partial t} = -h a_s (T_s - T_g) + R_c \Delta H_c - R_w \Delta H_w \quad (2)$$

Mass balance for gas:

$$\frac{\partial \dot{m}_g}{\partial z} = R_c + R_w \quad (3)$$

Mass balance for solids:

$$\frac{\partial \rho_s}{\partial t} = -R_c - R_w \quad (4)$$

Mass balance for carbon:

$$\frac{\partial C}{\partial z} = -R_c \quad (5)$$

Mass balance for moisture:

$$\frac{\partial W}{\partial t} = -R_w \quad (6)$$

Rate equation for coke combustion:

$$R_c = C A_c \exp\left(\frac{-E_c}{\Re T_s}\right) \quad (7)$$

Rate equation for moisture evaporation (Xianchun et al., 2009)

$$R_W = W A_w \exp\left(\frac{-E_w}{\Re T_s}\right) \quad (8)$$

Rate equation for moisture condensation (Porter & Easterling, 1992; McDonald, 1962)

$$R_W = W A_w \exp\left(\frac{-\Delta G^*}{\Re T_s}\right) \quad (9)$$

where,

$$\Delta G^* = \frac{16\pi\gamma^3 T_e^2}{3\Delta H_v^2 \Delta T^2} \quad (10)$$

Initial Condition:

At the top surface, the temperature of the solid is assumed at 1300°C, and the residual carbon is assumed to be zero due to complete burning. The rest of the solid bed is assumed at room temperature initially. The gas enters from the top surface at ambient temperature.

2.2. Discretized energy balance equations

The discretized energy balance equations based on explicit scheme for two major equations (1) and (2) are given by equations (11) and (12), respectively.

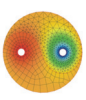

Discretized energy balance for gas phase

$$T^{l}_{g,i+1} = p_{a1}\left(\frac{hdz}{m^{l}_{g,i}C_{pg}}\right)T^{l}_{s,i} + \left(1 - P_{a1}\left(\frac{hdz}{m^{l}_{g,i}C_{pg}}\right)\right)T^{l}_{g,i} + P_{a4}\left(\frac{R^{l}_{W,i}\Delta H_{w}dz}{m^{l}_{g,i}C_{pg}}\right) \quad (11)$$

Discretized energy balance for solid

$$T^{l+1}_{s,i} = P_{a2}\left(\frac{hdt}{\rho^{l}_{s,i}C_{ps}}\right)T^{l}_{g,i} + \left(1 - P_{a2}\left(\frac{hdt}{\rho^{l}_{s,i}C_{ps}}\right)\right)T^{l}_{s,i} + P_{a3}\left(\frac{R^{l}_{c,i}\Delta H_{c}dt}{\rho^{l}_{s,i}C_{ps}}\right) - P_{a4}\left(\frac{R^{l}_{W,i}\Delta H_{w}dt}{\rho^{l}_{s,i}C_{pg}}\right) \quad (12)$$

There are four combined parameters to be optimized and each of which are assigned tuning factors, like p_{a1}, p_{a2}, p_{a3}, p_{a4}. Since the properties like heat transfer coefficient, gas flow rate, specific heats, bulk densities of solids will vary markedly above and below the fire line, the first two parameters (p_{a1}, p_{a2}) mentioned above are estimated for below and above the fire-line. The rate parameters of carbon combustion equation have been taken from literature (Ashley & Pradeep, 1998) but the overall rate has been adjusted using, p_{a3}. The rate parameters of evaporation and condensation have been taken from the literature (Xianchun et al., 2009; McDonald, 1962) and the overall rate has been adjusted using the adjustable factor p_{a4}

2.3. Methodology

The sinter model with governing equations and initial conditions are solved iteratively for all axial positions and time (Patankar, 1980). The GA calls this routine to calculate the fitness parameter for all its individual members. The GA model creates a population of individuals which are basically an array of process parameters to be optimized (Deb, 2001). Every individual is initiated with random values of parameters within their allowed range, all of which are feasible. The sinter model is solved for every individual and the predicted result is compared with that of the experimental values. This comparison of the predicted and experimental results gives the standard error which is used to define the fitness value of each individual; least error gives the highest fitness. The interaction of the two models occurs every time when this individual from GA model is passed to the sinter model and the error is sent from the sinter model to the GA model. This interaction of two models takes place for every individual in every generation of the GA model. After each generation, GA population is subjected to selection, mutation and crossover which direct the whole population towards the best solution in the search space while diversity is maintained through niching of the search space. The best individual of the whole run is chosen to be used as parameters in the sinter model.

3. RESULTS

For the present study the experimental data have been collected both from literature (Venkataramana et al., 1998) and experiments performed in the laboratory at RDCIS, SAIL, Ranchi, India, the details of which have been given in the authors' earlier publication (Giri & Roy, 2012). The optimized parameters obtained at different depths of the sinter bed, with and without consideration of moisture effects are tabulated in table 1.

Figure 1 shows the comparison of predicted temperature with experimental data at 190 mm depth (Giri & Roy, 2012) without considering the effect of moisture evaporation and condensation in the model. Figure 2 represents the similar curve while considering moisture evaporation and condensation. It is clearly observed that prediction in figure 2 is far better than prediction in figure 1. The deviations of predicted temperature from experimental data in case of figure 1, is towards initial and last stage of cooling as well as maximum temperature attained during heating. When evaporation is considered, moisture in the gas increases during preheating of solid that increases gas flow rate and the heat transfer efficacy from gas to solid, leading to enhanced solid temperature. This possibly explains better peak temperature prediction by figure 2. It is also observed that the temperature of the solid is under estimated during initial period of cooling in figure 1. This may possibly due to neglecting moisture condensation in the model, where gas releases heat to solid leading to condensation. Similarly, towards the end, figure 1 also underestimates the temperature of the solid.

***Table 1**. Optimized parameters at different depths.*

Moisture content	Moisture Consideration	Optimization depth	Optimization parameter					
			$p_{a1}(bf)$	$p_{a2}(bf)$	$p_{a1}(af)$	$p_{a2}(af)$	p_{a3}	p_{a4}
6%	Yes	190 mm	2.8191	5.4575	1.5206	3.5067	0.9166	0.3039
6%	No	190 mm	2.0808	6.2519	1.7355	4.4235	0.8597	
6.5%	Yes	300 mm	2.4095	6.6277	1.2003	3.5068	0.4818	0.0275
6.5%	No	300 mm	2.5197	9.9341	1.6689	4.6761	0.0479	
7.5%	Yes	385 mm	1.9992	2.6977	1.5275	2.2828	0.6313	4.86E-4
7.5%	No	385 mm	3.0769	5.0697	1.5350	2.4504	0.5260	

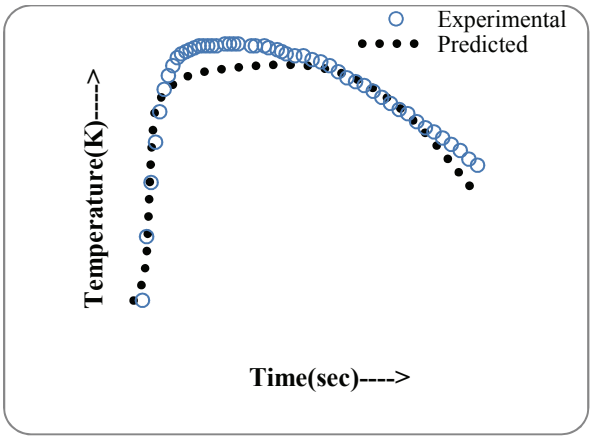

***Fig. 1.** Comparison of Predicted versus Experimental data at 190 mm depth without considering moisture effect in the model.*

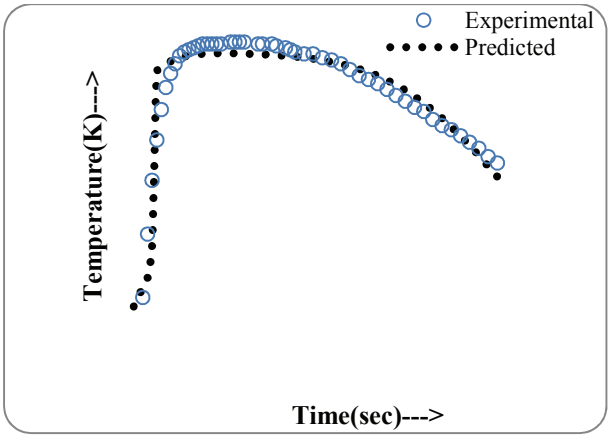

***Fig. 2.** Comparison of Predicted versus Experimental data at 190 mm depth considering the moisture effect in the model.*

In order to test some data with other moisture content, experimental data from literature (Venkataramana et al., 1998) were collected and used for validation of the model. Figure 3 shows the comparison of various predictions and the experimental data at 300 mm depth based on Venkataramana et al. (1998) data, shown as open symbols.

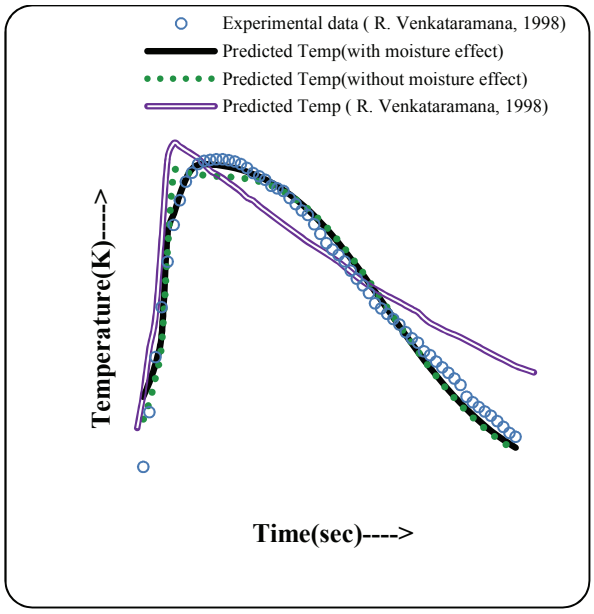

***Fig. 3.** Comparison of predicted versus experimental data at 300 mm depth.*

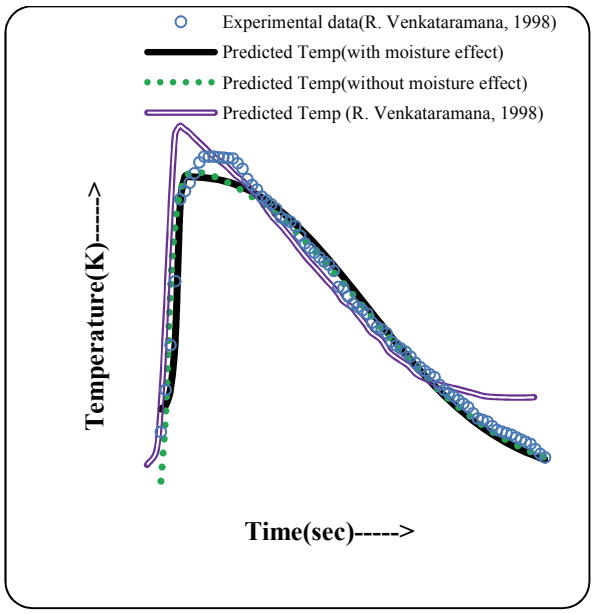

***Fig. 4.** Comparison of predicted versus experimental data at 385 mm depth.*

It is clearly observed that our predictions while considering the effect of moisture evaporation and condensation (indicated by solid line) closely matches with the experimental data.

Our prediction without considering moisture effect (indicated by dotted line) deviates from experimental data during the initial stage of cooling. It is also clear that both of our predictions are better than the prediction reported by Venkataramana et al. (1998), indicated by double lines. Similar plot is shown in figure 4 where experimental data has been taken from 385 mm depth and with initial moisture content of 7.5%. Here also our model predictions appear much better than predicted data reported in literature.

4. CONCLUSION

A mathematical model has been developed to predict the temperature profile in a fixed sinter bed. The model parameters have been estimated by employing GA. The effects of moisture evaporation and condensation have been taken into account in the phenomenological model. A significant improvement in the prediction of temperature profile has been observed when these phenomena are taken into consideration. This model can act as a potential tool for prediction of fire line progress in industrial sinter strand after tuning and mapping the optimized parameters against input parameters used there.

5. LIST OF SYMBOLS

a_s Specific surface area of the sinter bed, m^2/m^3
A_c frequency factor for carbon combustion rate equation, 1/sec
A_w frequency factor for moisture evaporation/condensation, 1/sec
C concentration of coke in the bed, kg/m^3
C_p specific heat of sintering gas/solid, J/kg-k
E_c activation energies for carbon combustion rate equation, J/mol
h gas-solid heat transfer co-efficient, $W/m^2 \cdot K$
ΔG^* free energy change to form the critical nucleus for condensation, J/mol
ΔH_c heat of combustion of coke, J/kg
ΔH_w latent heat of moisture evaporation/condensation, J/kg
$\dot{m}_g$ mass flow density of gas, kg/m^2-sec
$P_{a1,bf}, P_{a2,bf}$ adjustable parameters below the fire line, (-)
$P_{a1,af}, P_{a2,af}$ adjustable parameters after the fire line, (-)
P_{a3} adjustable parameter associated with the rate of carbon combustion, (-)
P_{a4} adjustable parameter associated with the rate of moisture evaporation and condensation, (-)
R_c rate of combustion of coke, $kg/m^3 \cdot sec$
R_w rate of moisture evaporation/condensation, $kg/m^3 \cdot sec$
T temperature of gas/solid, K
T_b boiling temperature of water, K
ΔT degree of supercooling, K
t time, s
W Concentration of moisture in solid, kg/m^3
ρ density, kg/m^3
R Universal gas constant, J/mol·K
z bed height from the top surface, m
γ surface tension of water, J/m

Subscript
i depth level below the top surface
g gas phase
s solid phase

Superscript
l time level

REFERENCES

Biswas, A.K., 1981, *Principles of Blast Furnace Ironmaking,* SBA Publication, Kolkata, India

Deb, K., 2001, *Multiobjective Optimization Using Evolutionary Algorithms*, John Wiley & Sons, Chichester, UK.

Giri B.K., Roy, G.G., 2012, Mathematical Modelling of Iron Ore Sintering Process using Genetic Algorithm, *Ironmaking & Steelmaking*, 39, 59-66

Ashley H.S., Pradeep A.K., 1998, Estimation of kinetic rate parameters for coal combustion from measurements of the ignition temperature, *Fuel*, 77, 1051-1059

McDonald, J.E., 1962, Homogeneous Nucleation of Vapor Condensation. I. Thermodynamic Aspects, *American J. Phys*., 30, 870-877

Patankar, S.V., 1980, *Numerical heat transfer and fluid flow*, Hemisphere Publishing Corporation, New York.

Porter, D.A., Easterling, K.E., 1992, *Phase Transformation in Metals and Alloys*, Chapman & Hall, London.

Venkataramana, R., Gupta, S.S., Kapur P.C., Ramchandran, N., 1998, Mathematical Modelling and Simulation of the Iron Ore Sintering Process, *Tata Search*, 50-54

Xianchun, L.I., Hui, S., Qi, W., Chatphol, M, Terry, W., Jianglong, Y.U., 2009, Experimental Study on drying and moisture re-absorption Kinetics of an Indonesian Low rank Coal, *J. Environ Sci.,* 21, S127-S130

MATEMATYCZNE MODELOWANIE PROCESU SPIEKANA RUDY ŻELAZA PRZY WYKORZYSTANIU ALGORYTMU GENETYCZNEGO: WPŁYW ODPAROWANIA I SKRAPLANIA WILGOCI NA PROFIL TEMPERATURY

Streszczenie

Spiekanie jest procesem, w którym rozdrobniona/oczyszczona ruda żelaza jest gromadzona w formie spieczonej bryły w wyniku częściowej fuzji w obecności paliwa i topnika. Proces spiekania wsadu rozpoczyna się od góry, przy czym płomień przemieszcza się w dół w wyniku wymuszonego ruchu powietrza. Oszacowanie prędkości poruszania się płomienia w głąb wsadu jest istotne, ponieważ wydajność taśmy spiekalniczej zależy od momentu kiedy płomień osiąga dno wsadu. W artykule opisano matematyczny model procesu spiekania rudy żelaza w ruszcie spiekalniczym. Ponadto zastosowano algorytm genetyczny, który w połączeniu z modelem procesu pozwala oszacować optymalne parametry procesu spiekania. Obecność wilgoci wpływa znacząco na temperaturę spiekania, ponieważ parowanie i skraplanie kontrolują zarówno temperaturę jak i, co

najważniejsze, szybkość przepływu płomienia (gazu) w wsadzie. Niniejsza praca jest modyfikacją opracowanego przez tych samych autorów modelu, w którym skraplanie i odparowywanie wilgoci wprowadzono do modelu spiekania by w sposób jawny wytłumaczyć wpływ wilgoci. Wyniki dla zmodyfikowanego modelu wskazują na znaczną poprawę przewidywań modelu w przypadku, gdy uwzględniane są czynniki odparowywania i skraplania wilgoci.

Received: : September 22, 2012
Received in a revised form: October 8, 2012
Accepted: October 10, 2012